Journal of Biomolecular Structure and Dynamics

ISSN: (Print) (Online) Journal homepage: https://www.tandfonline.com/loi/tbsd20

Cefmetazole sodium as an allosteric effector that regulates the oxygen supply efficiency of adult hemoglobin

Peilin Shu, Guoxing You, Weidan Li, Yuzhi Chen, Zongtang Chu, Dong Qin, Ying Wang, Hong Zhou & Lian Zhao

To cite this article: Peilin Shu, Guoxing You, Weidan Li, Yuzhi Chen, Zongtang Chu, Dong Qin, Ying Wang, Hong Zhou & Lian Zhao (09 Aug 2023): Cefmetazole sodium as an allosteric effector that regulates the oxygen supply efficiency of adult hemoglobin, Journal of Biomolecular Structure and Dynamics, DOI: 10.1080/07391102.2023.2245043

To link to this article: https://doi.org/10.1080/07391102.2023.2245043

JOURNAL OF BIOMOLECULAR STRUCTURE AND DYNAMICS
https://doi.org/10.1080/07391102.2023.2245043

Cefmetazole sodium as an allosteric effector that regulates the oxygen supply efficiency of adult hemoglobin

Peilin Shu, Guoxing You, Weidan Li, Yuzhi Chen, Zongtang Chu, Dong Qin, Ying Wang, Hong Zhou and Lian Zhao

Institute of Health Service and Transfusion Medicine, Academy of Military Medical Sciences, Academy of Military Science of the Chinese People's Liberation Army, Beijing, P.R. C

Communicated by Ramaswamy H. Sarma

ABSTRACT

Allosteric effectors play an important role in regulating the oxygen supply efficiency of hemoglobin for blood storage and disease treatment. However, allosteric effectors that are approved by the US FDA are limited. In this study, cefmetazole sodium (CS) was found to bind adult hemoglobin (HbA) from FDA library (1338 compounds) using surface plasmon resonance imaging high-throughput screening. Using surface plasmon resonance (SPR), the interaction between CS and HbA was verified. The oxygen dissociation curve of HbA after CS interaction showed a significant increase in P_{50} and theoretical oxygen-release capacity. Acid-base sensitivity (SI) exhibited a decreasing trend, although not significantly different. An oxygen dissociation assay indicated that CS accelerated HbA deoxygenation. Microfluidic modulated spectroscopy showed that CS changed the ratio of the alpha-helix to the beta-sheet of HbA. Molecular docking suggested CS bound to HbA's β-chains *via* hydrogen bonds, with key amino acids being N282, K225, H545, K625, K675, and V544.The results of molecular dynamics simulations (MD) revealed a stable orientation of the HbA-CS complex. CS did not significantly affect the P_{50} of bovine hemoglobin, possibly due to the lack of Valβ1 and Hisβ2, indicating that these were the crucial amino acids involved in HbA's oxygen affinity. Competition between the 2,3-Diphosphoglycerate (2,3-DPG) and CS in the HbA interaction was also determined by SPR, molecular docking and MD. In summary, CS could interact with HbA and regulate the oxygen supply efficiency *via* forming stable hydrogen bonds with the β-chains of HbA, and showed competition with 2,3-DPG.

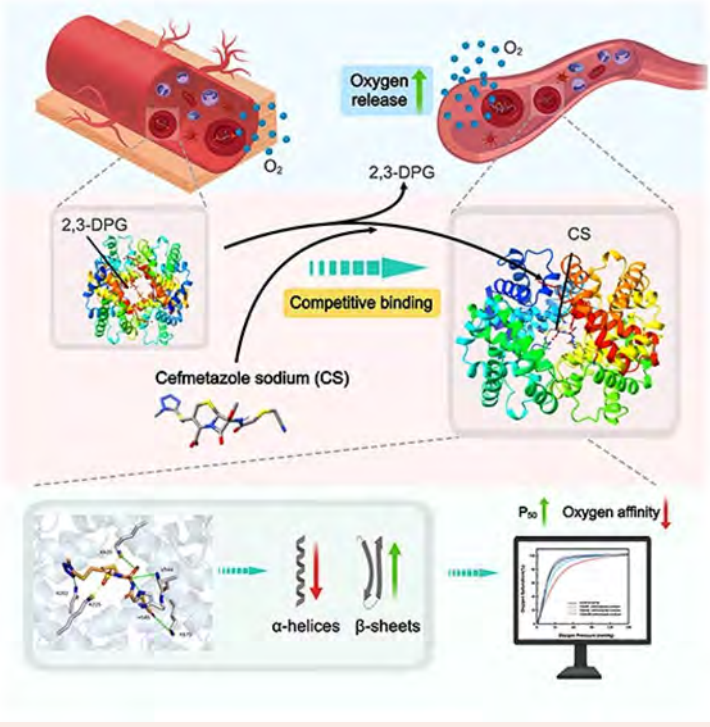

ARTICLE HISTORY
Received 15 March 2023
Accepted 17 July 2023

KEYWORDS
Hemoglobin oxygen affinity; P_{50} value; allosteric effect; cefmetazole sodium

CONTACT Ying Wang wy830111@163.com; Hong Zhou zhouhtt1966@163.com; Lian Zhao zhaolian@bmi.ac.cn
This article has been corrected with minor changes. These changes do not impact the academic content of the article.

Introduction

Hemoglobin plays an important role in carrying and transporting oxygen molecules into tissues to maintain metabolic activity (Giardina et al., 1995). The oxygen demands of the human body require a constant circulation of blood with a high concentration of hemoglobin. Hemoglobin accounts for approximately 1% of the body weight of humans (Bellelli & Tame, 2022). This substantial amount of protein is essential for meeting the oxygen requirements of the body's tissues.

The function of hemoglobin is closely related to its structural characteristics. Hemoglobin is a heterotetramer consisting of two α-subunits and two β-subunits, each of which link a central heme group consisting of an iron ion and a porphyrin ring (Hill et al., 1962). Each heme group can bind an oxygen molecule. X-ray crystal diffraction has revealed that there are two distinct quaternary states of hemoglobin called the 'T' state, for "tense", and 'R' state, for "relaxed". Hemoglobin in the 'T' state exhibits low oxygen affinity and releases oxygen easily. Hemoglobin in the 'R' state exhibits high oxygen affinity and combines easily with oxygen (Perutz et al., 1998; Safo et al., 2011; Perutz & TenEyck, 1972). Molecular cooperativity is one of the distinctive characteristics of hemoglobin, and it is responsible for the sigmoid shape observed in the oxygen dissociation curve (ODC) (refer to Figure 1) (Carreau et al., 2011; Srinivasan et al., 2017). Cooperativity is expressed by the Hill coefficient, which is the maximal slope of the ODC in the Hill-plot (Mairbäurl & Weber, 2012). The oxygen partial pressure corresponding to 50% oxygen saturation (P_{50}) from the ODC is used as an indicator to characterize the oxygen affinity of hemoglobin. The Bohr effect describes the increased oxygen affinity of hemoglobin because of the decreased partial pressure of carbon dioxide and/or increased pH (Benner et al., 2022; Kaufman et al., 2022). The strength of the Bohr effect is mainly characterized by the acid-base sensitivity index (SI), which is evaluated from the variation range of the P_{50} value under different acid-base environments. In addition, the difference in oxygen saturation (ΔSO_2) between the simulated lung and tissue cells on the ODC is defined as the theoretical oxygen-release capacity, which mainly reflects the ability of blood for supplying oxygen to tissue cells under different environment. The oxygen affinity, cooperativity, Bohr effect, and the theoretical oxygen-release capacity enable hemoglobin to carry and release oxygen. In the present study, these four parameters were used to characterize the oxygen supply efficiency of hemoglobin.

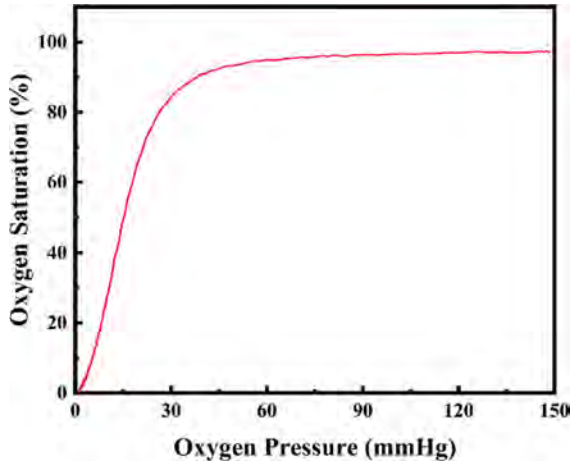

Figure 1. The oxygen dissociation curve (ODC) describes the relationship between the partial pressure of oxygen (pO_2) and the saturation of HbA with oxygen. The P_{50} value represents the specific pO_2 at which hemoglobin is 50% saturated with oxygen.

The conformation of hemoglobin has been reported to possibly be regulated, which results in a variation in the oxygen supply efficiency that further affects the oxygen uptake and use in humans. Many endogenous molecules, called allosteric effectors, play the key role in altering the hemoglobin conformation. The main endogenous allosteric effectors of hemoglobin are H^+, CO_2, and 2,3-Diphosphoglycerate (2,3-DPG). H^+ mainly binds to the α1Val, β82 Lys, and β146 His residues of adult hemoglobin (HbA). CO_2 can bind to the *N*-terminal residues of the α- and β-chains of HbA to form a carbamate. With increasing H^+ and CO_2 concentrations, the oxygen affinity of HbA decreases and the released oxygen increases. A product of erythrocyte glycolysis, 2, 3-DPG, can bind to multiple sites on the β-chain of HbA to form salt bonds, which stabilize the HbA structure and cause the HbA to transit from the 'R' state to the 'T' state, resulting in reduced oxygen affinity. The 2, 3-DPG levels are physiologically elevated in anemia patients and in people who rapidly move to high altitudes (plateaus; for 3–7 days) (Srinivasan et al., 2017; Mairbäurl & Weber, 2012; Malte & Lykkeboe, 2018; Li et al., 2018).

Hypoxemia can affect the oxygen supply, and thus the regulation of hemoglobin oxygen affinity is manipulated in clinical settings, such as the blood storage and disease treatments. The P_{50} value of stored red blood cells has shown to decrease from 27 mmHg (fresh blood) to 18 mmHg after 21 days of storage (Li et al., 2016). Valeri and Zaroulis have developed a technique to rejuvenate red blood cells. The P_{50} value was significantly improved after rejuvenation, which effectively reduced the potential for organ damage caused by the infusion of old blood in White-landrace pigs (Woźniak et al., 2018). Sickle cell disease (SCD) is an inherited disorder that affects millions of people worldwide. In situations of low oxygen levels, sickle hemoglobin (HbS) can aggregate and distort red blood cells, causing them to assume a rigid sickle shape. This abnormal shape then leads to hemolysis, occlusion and thrombosis in small blood vessels (Eaton & Hofrichter, 1990; Bunn, 1997; Rees et al., 2010). GBT440 (voxelotor) can bind to HbS to increase the oxygen affinity and prevent the polymerization of HbS. In 2019, voxelotor was approved by the US Food and Drug Administration (FDA) for the treatment of SCD in adults and pediatric patients aged ≥ 12 years (Blair, 2020). RSR-13 and myo-inositol trispyrophosphate (ITPP) are allosteric effectors that reduce the oxygen affinity of hemoglobin and facilitate the release of oxygen. When used as an adjunctive chemotherapy agent, ITPP reduced the tumor size and improved survival in rat models of hepatocellular (Aprahamian et al., 2011) and pancreatic (Raykov et al., 2014) carcinoma, as well as in mouse models of primary (Derbal-Wolfrom et al., 2013) and metastatic colorectal cancer (Limani et al., 2016). Targeting the oxygen

affinity of hemoglobin to regulate oxygen supply efficiency has many applications.

Despite these results, our knowledge about the use of allosteric effectors for regulating hemoglobin oxygen affinity is still limited. Apart from GBT440, most of the existing allosteric effectors have failed to be approved by FDA. The reasons were as follows: IHP could not cross cell membranes easily and TD-1 was insoluble in water (Fylaktakidou et al., 2005; Nakagawa et al., 2018). Therefore, research on these effectors is lacking. Another effector, 5-HMF, was discontinued in phase II clinical trials for SCD because of low bioavailability *in vivo* (Ahmed et al., 2020). A phase III study of 515 patients with brain metastases found that treatment with RSR-13 resulted in a modest but insignificant increase in survival and further investigation of the treatment was discontinued (Srinivasan et al., 2017; Suh et al., 2006). GBT440, the only allosteric effector approved by the FDA, has been reported to have no special effects on normal hemoglobin. Thus, the further research of allosteric effectors is desirable.

In addition, understanding the intricate mechanisms of interaction between drugs and proteins is crucial for conducting effective research (Khashkhashi-Moghadam et al., 2022; Taheri et al., 2022). The methods utilized to assess the interaction between small molecules and proteins include Surface Plasmon Resonance (SPR) and Microfluidic Modulated Spectroscopy (MMS). Molecular docking and molecular dynamics simulations (MD) are also extensively utilized to analyze the interactions, elucidating the mechanistic and dynamic aspects at the molecular level (Sharifi-Rad et al., 2021; Assaran Darban et al., 2017).

In the present study, we performed surface plasmon resonance imaging (SPRi) high-throughput screening to identify molecules capable of binding to HbA from an FDA library of 1338 compounds. Then, SPR was used to determine the actual interaction between the screened compound, cefmetazole sodium, and HbA. We explored the effect of cefmetazole sodium on the oxygen supply efficiency and oxygen release rate of HbA. MMS showed that effect of cefmetazole sodium on the secondary structure of HbA. Furthermore, molecular docking analysis was used to indicate the binding site. The binding stability of cefmetazole sodium to HbA was determined by MD. The amino acid sequences of bovine hemoglobin (bHb) and HbA were compared to explain the different effects of cefmetazole sodium on the oxygen affinity of them. We also determined the competition between the endogenous substance, 2,3-DPG, and cefmetazole sodium in the interaction with HbA.

Materials and methods

Preparation of HbA

Volunteers' blood was withdrawn through the median cubital vein. HbA was purified from whole blood mixed with CPDA-1 (Sigma Aldrich, St Louis, MO, USA) by anion-exchange chromatography and was prepared at a concentration of 5 g/dL, as previously described (Chu et al., 2020).

Identification of compounds that bind to HbA using surface plasmon resonance imaging technology (SPRi)

An SPRi instrument (Kx5; Plexera; Beijing,China) was used to monitor the interactions between the compounds and HbA. Compounds from an FDA library ($n = 1338$) were printed on a three-dimensional (3D) optical cross-linked chip. The chip was vacuum dried, and an optical cross-linking reaction was carried out. The HbA was diluted to concentrations of 14, 70, and 350 μM with PBS (pH = 7.4) buffer and used as the mobile phase component in the experiment. On the surface of the chip, the current phase flow rate was 2 μL·s^{-1}, the binding time and the disintegration time were 300 s, respectively. Glycine-HCl solution (pH = 2.0) was used as the regeneration fluid at a flow rate of 2 μL·s^{-1} for 300 s. Samples were monitored and analyzed in real time *via* the Plexarray HT biomolecular interaction analyzer in the SPR V3 version (Plexera SPR Data Analysis Model; Plexera) (Xu et al., 2019).

Identification of the interaction between cefmetazole sodium and HbA using surface plasmon resonance technology (SPR)

The interaction between cefmetazole sodium (Solarbio; Beijing, China) and HbA at room temperature was determined using SPR instruments (Nicoya Life Science, Inc., Kitchener, Canada). A carboxyl sensor chip was installed on the SPR instrument. HbA was diluted to 5 μg/μL with immobilization buffer (10 mM sodium acetate, pH 4.5). The activation buffer was prepared by mixing 400 mM 1-(3-dimethylaminopropyl)-3-ethylcarbodiimide hydrochloride (Sigma Aldrich) and 100 mM *N*-hydroxysuccinimide (Sigma Aldrich) immediately prior to injection for 4 min, which activated HbA by coupling with carboxyl groups. Then, ethanolamine hydrochloride (1 M; blocking solution) was added (20 μL/min, 4 min). Finally, the multi-cycle method was used for analysis. Cefmetazole sodium was diluted to 6400, 3200, 1600, 800, 400, and 0 μM with PBS and injected at a flow rate of 20 μL/min for an association of 240 s, followed by dissociation for 480 s. The association and dissociation processes were performed in the running buffer 1 × HEPES (10 mM HEPES, 150 mM NaCl, and 3 mM EDTA, with 0.005%Tween-20, pH 7.4). The binding reactions' kinetic parameters were calculated using Trace Drawer software (Ridgeview Instruments AB, Sweden) (Zhong et al., 2021; Dybas et al., 2020).

The binding between the mixture of 2,3-DPG (Sigma Aldrich) and cefmetazole sodium and HbA was also determined by this method.

Investigation of the effects of cefmetazole sodium on the oxygen supply efficiency via the ODC

Cefmetazole sodium at concentrations of 0, 15, 50, and 150 mM was incubated with HbA for 30 min. The obtained samples were diluted in 4 mL of BLOODOX-Solution buffer with pH values of 7.2, 7.4, and 7.6, mixed with 20 μL of bovine serum albumin (20%, Sigma Aldrich) and 20 μL of anti-foaming agent (Sigma Aldrich) (Chu et al., 2020). Next,

the samples were analyzed using a BLOODOX-2018 analyzer (Softron Biotechnology, Beijing, China) (Chu et al., 2020). The ODC was recorded and the P_{50} values and Hill coefficients were obtained. The SI was calculated as follows: $SI = (P_{50(pH = 7.2)} — P_{50\ (pH = 7.6))}/P_{50(pH = 7.4)}$ (Yuan et al., 2015). Then, the ΔSO_2 value of HbA in simulated plain and plateau environments (6000 m) after binding cefmetazole sodium was calculated. The formula was as follows:

$$\Delta SO_{2(100–40\ mmHg)} = SO_{2(100\ mmHg,\ pH=7.6)} – SO_{2(40mm\ Hg,\ pH=7.2)}$$

$$\Delta SO_{2(60–30\ mmHg)} = SO_{2(60\ mmHg,\ pH=7.6)} – SO_{2(30\ mmHg,\ pH=7.2)}.$$

where $\Delta SO_{2(100–40\,mmHg)}$ represents the theoretical oxygen-release capacity of HbA in the plain environment and $\Delta SO_{2(60–30\,mmHg)}$ represents the theoretical oxygen-release capacity of HbA in the plateau environment; $SO_{2(100\,mmHg,\ pH\ =\ 7.6)}$ and $SO_{2(60\,mmHg,\ pH\ =\ 7.6)}$ represents the HbA oxygen saturation at pH 7.6 and an oxygen partial pressure of 100 mmHg and 60 mmHg, which simulates the environment in the lung under plain and plateau conditions; $SO_{2(40\,mmHg,\ pH\ =\ 7.2)}$ and $SO_{2(30\,mmHg,\ pH\ =\ 7.2)}$ represents the HbA oxygen saturation at pH 7.2 and an oxygen partial pressure of 40 mmHg and 30 mmHg, which simulates the environment in peripheral tissues under plain and plateau conditions.

Detecting the effect of cefmetazole sodium on the oxygen release from HbA using the oxygen dissociation assay (ODA)

The ODA is used to measure the oxygen release during the deoxygenation process of HbA. HbA (1 mg) was incubated in the presence of cefmetazole sodium (150 mM) or GBT440 (4.4 mM; Topscience, USA,) for 30 min at room temperature. Then, the samples were diluted with 4 mL of BLOODOX-Solution buffer and deoxygenated with gaseous dry N_2 at 20 L/min for 2 h at 37 °C in FLUO star Omega (BMG Labtech, Inc., Ortenberg, Germany). An ultraviolet/visible (UV/Vis) absorbance spectrometer was used to record the spectra (350–600 nm, with a resolution of 1 nm) of samples in <1 s/well during deoxygenation for 2 h (20 cycles) (Patel et al., 2018).

Determination of the effect of cefmetazole sodium on the higher order structure (HOS) of HbA by Microfluidic modulation spectroscopy (MMS)

The effect of cefmetazole sodium on the secondary structures of HbA was evaluated using modulation spectroscopy (MMS), an innovative automated infrared (IR) technique that has demonstrated its ability to reliably generate high-quality secondary structure data for proteins (Ivancic et al., 2022). The samples were analyzed using the AQS3®pro MMS production system (RedShiftBio, Burlington, MA, USA). All samples and their corresponding buffer solutions were preloaded in a pairwise manner onto a 24-well plate and introduced into the microfluidic transmission cell by applying compressed air at 5 psi, and modulated at a frequency of 1 Hz as they passed through the laser path. The original absolute absorption spectra of the samples were obtained in the range of 1701–1598 cm^{-1} and converted into the second derivative plot to highlight. Then the characteristic peaks of the second order structure was identified. The HOS components, alpha-helix (Alpha), beta-sheet (Beta), unordered, and beta-turn (Turn), were calculated using the same baseline-corrected plot and Gaussian curve fitting method. The analysis and spectral processing of the samples were performed using the AQS3® delta control software.

Determination of the interaction between cefmetazole sodium and HbA via molecular docking analysis

Molecular docking was conducted to ascertain the potential binding sites between cefmetazole sodium and HbA. The 3D structures of HbA and cefmetazole sodium were downloaded from the Protein Data Bank [PDB ID: 1B86] and PubChem [CID: 23666711], respectively. The docking analysis of HbA and cefmetazole sodium was conducted using AutoDock 4.2 software, and the ligand binding energy within the conformational search space was evaluated utilizing the Lamarckian genetic algorithm provided by the software. The AutoDock tool was used for the removal of water molecules and addition of polar hydrogen atoms in HbA. The amino acid residues surrounding the active site of HbA were used to form a larger range of Box, and then different types of atoms were used as probes to scan and calculate the grid energy, which was processed by the AutoGrid program. 2,3-DPG was docked onto the phosphate binding site of the HbA protein (PDB: 1B86) using AutoDockVina and the Root Mean Square Deviation (RMSD) value was calculated to validate the docking protocol. In the docking development, 100 conformations were considered for cefmetazole sodium. The minimal binding free energy conformer was used for further analysis. The PyMOL software package was used for illustration of the docked conformations.

The same method as described above was used to reveal the competitive nature of the binding of 2,3-DPG and cefmetazole sodium with HbA. The 3D structure of 2,3-DPG was downloaded from PubChem [CID: 61].

The binding stability of cefmetazole sodium to HbA was determined by molecular dynamic simulation

The molecular dynamic simulation of the Autodock vina docking complex was performed using AMBER 20 program. High-quality atomic charges of ligand were generated by AM1-BCC model. The solvation model used for molecular dynamics simulation was OPC. 10 Å truncated octahedron box has been used as boundary conditions. The topology and coordinate files were subsequently created for molecular dynamic simulation. The non-bonded cutoff is 10 Å. The systems were then minimized for 5000 energy steps while restraining the heavy atoms of HbA and cefmetazole sodium, in order to relax the hydrogens, water molecules, and salt ions. Then, 5000 steps of minimization were performed while restraining the HbA backbone. Then, the restrains were removed and the entire system was minimized for another 20000 steps. The systems were then thermalized from 0 to 300 K using the canonical NVT ensemble (number volume temperature) at 1.0 atm for 20 ps (Sharifi-Rad et al., 2021). The heated systems were then equilibrated at

300 K for 200 ps with restraint at 1.0 atm under isothermal–isobaric ensemble (NPT) conditions using Langevin thermostat. Another 1 ns equilibration in NVT system using Berendsen thermostat. Production of 100 ns was then performed and 5,000 snapshots generated for MM/GBSA calculations (Li et al., 2011). MM/GBSA method employed to calculate the binding energies averaged over 5,000 snapshots in Amber 20. The 2D diagram was drawn by Discovery Studio 4.5 Client.

The binding stability of 2,3-DPG to HbA was also determined by this method.

Statistical analysis

Data are expressed as mean ± standard deviation (SD). Statistical analysis was performed using SPSS 9.2 (IBM, SPSS statistics 22). The plots displayed in the study represent the mean data from at least three experiments. All data were analyzed with a normality test. One-way independent ANOVA was used for comparison between different groups. $^{*}p < 0.05$ and $^{**}p < 0.01$ indicate statistical significance.

Results

Identification of the binding between cefmetazole sodium and HbA

The data showed that the SPRi response increased with increasing HbA concentration (14, 70, and 350 μM) (Figure 2b). By detecting the change in SPR angle, kinetic information (KD, K_d and K_a) was calculated (Figure 2c). KD (K_d/K_a) represents the degree of dissociation of the receptor–ligand complex at equilibrium, and as the value for KD decreases, the affinity increases. The KD value of cefmetazole sodium interacting with HbA was 5.82×10^{-4}. The results also showed that the combination between cefmetazole sodium and HbA was concentration dependent (Figure 2d).

The effect of cefmetazole sodium on the oxygen supply efficiency of HbA

The P_{50}, Hill coefficient, SI, and ΔSO_2 values were determined, which together characterize the oxygen supply efficiency of HbA. After incubating with cefmetazole sodium, ODC of HbA shifted to the right (Figure 3a), indicating a significant increase in the P_{50} value. The P_{50} value of HbA was 13.65 ± 1.93 mmHg. When incubated with cefmetazole sodium, the P_{50} value was increased to 15.17 ± 1.56 mmHg (15 mM cefmetazole sodium), 15.95 ± 1.99 mmHg (50 mM cefmetazole sodium), and 22.78 ± 3.90 mmHg (150 mM cefmetazole sodium, $p < 0.01$ vs. 0 mM; $p < 0.05$ vs. 15 and 50 mM) (Figure 3b). The impact of cefmetazole sodium on the P_{50} value of HbA displayed a dose-dependent relationship. In addition, with increasing cefmetazole sodium concentrations, the Hill coefficient gradually decreased. The Hill coefficient of HbA was 2.24 ± 0.26. After incubation with cefmetazole

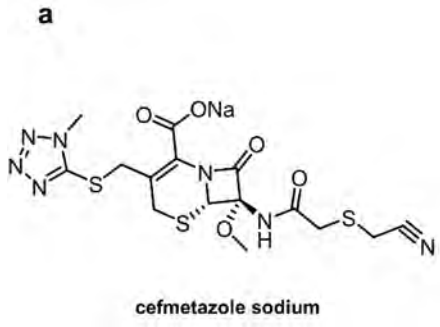

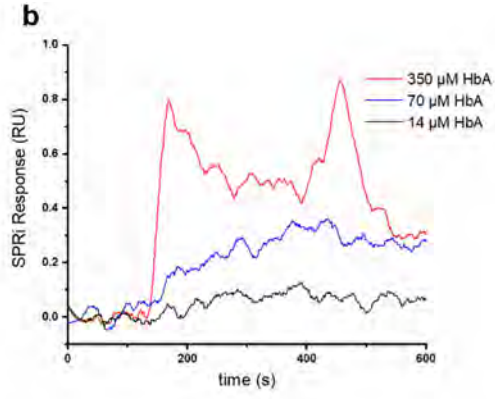

c

Parameter	Result
Ka (1/M*S)	6.07×10^{-1}
Kd (1/S)	3.53×10^{-2}
KD (M)	5.82×10^{-4}

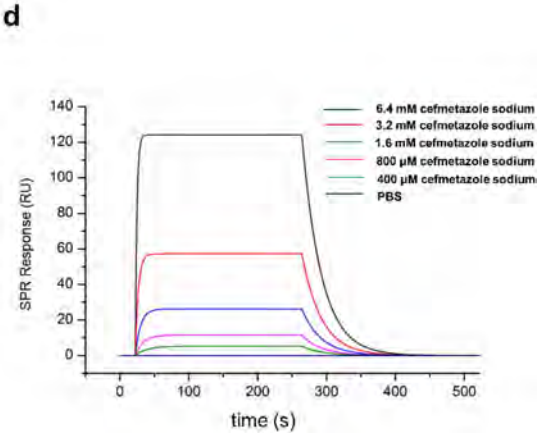

Figure 2. Surface plasmon resonance imaging (SPRi) and surface plasmon resonance (SPR) indicated there was an interaction between cefmetazole sodium and HbA. (a) The chemical structure of cefmetazole sodium. (b) Gradient binding curve of cefmetazole sodium and HbA at different concentrations in the SPRi assay. (c) Dynamics and affinity parameters of cefmetazole sodium binding to HbA. (d) Cefmetazole sodium bound to HbA in a dose-dependent manner in the SPR assay.

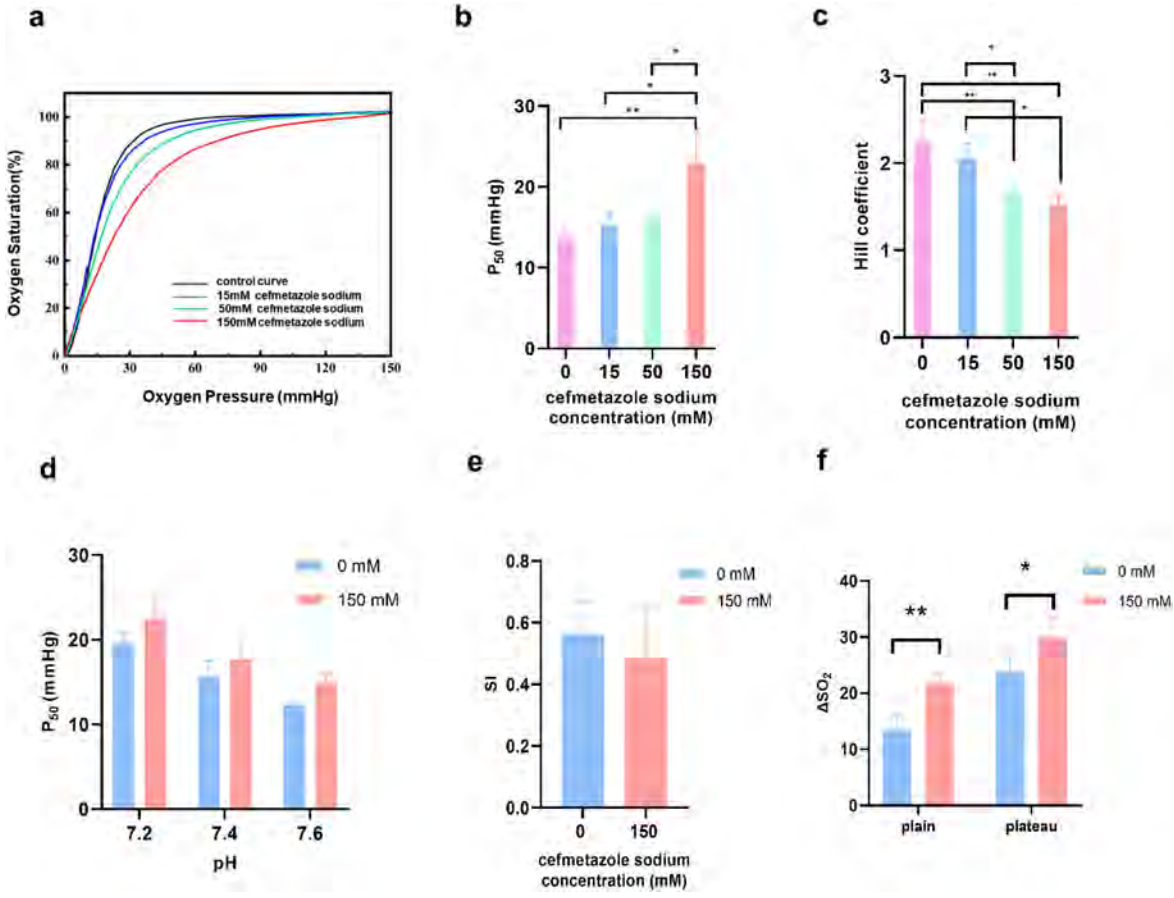

Figure 3. Cefmetazole sodium can regulate the oxygen supply efficiency of HbA. (a) The oxygen dissociation curve (ODC) of HbA mixed with cefmetazole sodium (0, 15, 50, and 150 mM). cefmetazole sodium shifted the ODC to the right. (b) The P_{50} value of HbA mixed with cefmetazole sodium (0, 15, 50, and 150 mM). cefmetazole sodium significantly increased the P_{50} value of HbA at a concentration of 150 mM. (c) The effect of cefmetazole sodium on the Hill coefficient of HbA. The Hill coefficient of HbA was significantly reduced by addition of 50 and 150 mM cefmetazole sodium. (d) Cefmetazole sodium had no effect on the Bohr effect of HbA. (e) Cefmetazole sodium did not significantly change the acid-base sensitivity index (SI) of HbA. (f) Cefmetazole sodium increased the theoretical oxygen-release capacity of HbA under simulated plain and plateau conditions. Error bars represent the standard deviation (SD). * indicates $p < 0.05$, * * indicates $p < 0.01$.

sodium, the Hill coefficient of HbA decreased to 2.06 ± 0.18 (15 mM cefmetazole sodium), 1.67 ± 0.12 (50 mM cefmetazole sodium, $p < 0.01$ vs. 0 mM; $p < 0.05$ vs. 15 mM), and 1.52 ± 0.12 (150 mM cefmetazole sodium, $p < 0.01$ vs. 0 mM; $p < 0$. 05 vs. 15 mM) (Figure 3c). The P_{50} value of HbA decreased with an increase in the pH value, but the decrease was not significant with or without cefmetazole sodium (Figure 3d). The SI decreased slightly from 0.56 ± 0.11 to 0.48 ± 0.17 after incubation with 150 mM cefmetazole sodium ($p > 0.05$) (Figure 3e). In addition, 150 mM cefmetazole sodium increased the theoretical oxygen-release capacity of HbA from 15.51% ± 6.45% to 21.53% ± 2.27% in the simulated plain environment ($p < 0.01$) and from 25.42%±5.85%to 28.94%±4.31% in the simulated plateau environment ($p < 0.05$, Figure 3f).

Cefmetazole sodium accelerates the oxygen release of HbA

Figure 4 shows the spectra of HbA samples during deoxygenation for 2 h (20 cycles). The Soret peak (414 nm) shifting to the right indicated the deoxygenation of HbA (Coll-Satue et al., 2021). The more the Soret peak shifts to the right, the higher the level of deoxyhemoglobin in the samples and the faster the release of oxygen from HbA. The results showed that the Soret peak of HbA shifted from 414 to 416 nm after 20 cycles. After incubating with GBT440, a compound known to reduce the P50 value of HbA, a noticeable shift in the Soret peak of HbA was observed from 414 nm to 415 nm (Figure 4a, b). However, the Soret peak of HbA in the present of cefmetazole sodium shifted from 414 to 418 nm during deoxygenation (Figure 4c, d). Therefore, the presence of cefmetazole sodium resulted in more deoxygenated HbA during deoxygenation for 2 h, which suggested cefmetazole sodium accelerated the oxygen release from HbA.

Cefmetazole sodium changes the HOS of HbA

Figure 5a displays the absolute absorption spectra and second derivative spectra of HbA, acquired the spectral range of 1701–1598 cm^{-1}. 1652 cm^{-1} was the most intense, which indicats that HbA existed in α-helix-rich conformation chiefly. Figure 5b showed the overall similarity score was 99.75% for the HbA and 99.80% for the HbA with cefmetazole sodium (150 mM), which indicates excellent system stability. Figure 5c showed that cefmetazole sodium-HbA complex is significantly different from the HbA, and the similarity is only 86.38%. The HOS bar chart results in Figure 5d

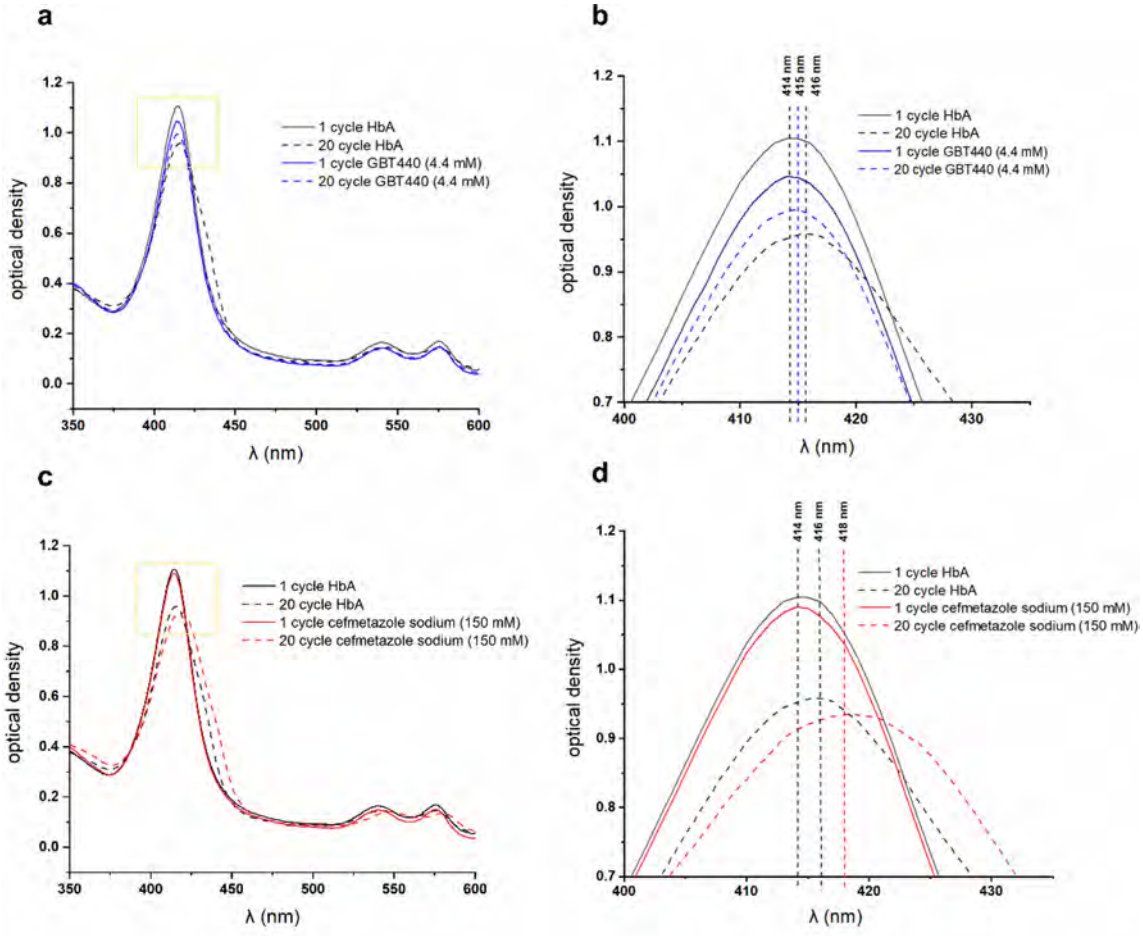

Figure 4. Cefmetazole sodium accelerated the oxygen release from HbA. (a) The spectra of HbA, with and without GBT440, with scanning from 350 nm to 600 nm. (b) The magnified view of the yellow frame in (a) from 400 nm to 430 nm. GBT440 slowed down the rate of oxygen release from HbA. (c) The spectra of HbA, with and without, cefmetazole sodium with scanning from 350 nm to 600 nm. (d) The magnified view of the yellow frame in (c) from 400 to 430 nm. Cefmetazole sodium accelerated the oxygen release from HbA.

showed that cefmetazole sodium changed the secondary structure of HbA. The alpha-helix and beta-sheet structures of HbA are notably affected to the greatest extent. Cefmetazole sodium causes a significant reduction in the alpha-helix content of HbA from 76.24% to 67.33% and a significant increase in the beta-sheet content of HbA from 5.71% to 14.64%. In addition, cefmetazole sodium reduces beta-turns (turn) of HbA from 5.31% to 3.81% and increases the unord of HbA from 12.74% to14.22%.

Cefmetazole sodium binds to N282, K225, H545, K625, K675 and V544 of HbA

A comparison was made between the docked conformation of 2,3-DPG and the original crystal structure of 2,3-DPG, resulting in a calculated RMSD value of 1.006 Å. The binding orientations of the 100 docked conformations of cefmetazole sodium are shown in Figure 6a. The docked conformations with the lowest free energy were chosen for further analysis (Figure 6b). Cefmetazole sodium could flexibly match and combine with the active pocket of HbA, and the binding energy was −7.32 kcal/mol. Further analysis showed that cefmetazole sodium bound in the central hydrophobic cavity within the two β-chains of HbA (Figure 6b). The key amino acids in the β-chain that contributed to the ligand binding were N282, K225, H545, K625, K675 and V544. Specifically, the β-lactam scaffold of cefmetazole sodium fitted well into the binding pocket of HbA and the carboxylic acid group formed Salt bridge interaction with the NH groups of K625 and K225. The carbonyl on the azabicyclo[4.2.0] core of cefmetazole sodium formed a hydrogen bond with the NH of H545. The methoxy group on the azabicyclo[4.2.0] core formed a hydrogen bond with the NH of V544. Additionally, the nitrogens at the 3- and 4-positions of the tetrazole moiety formed one hydrogen bonds with the NH of N282 (Figure 6c).

Cefmetazole sodium and HbA form a stable complex

To evaluate the stability of the systems RMSD values of the protein backbone in HbA and HbA-cefmetazole sodium complex were calculated. The RMSD plot of HbA and HbA-cefmetazole sodium complex is illustrated in Figure 7a. The RMSD value of cefmetazole sodium undergoes significant changes during the first 40 ns of molecular simulation, indicating a large positional variation of cefmetazole sodium during this initial 40s period. After 50 ns of simulation, the RMSD was found to attain stability in their respective

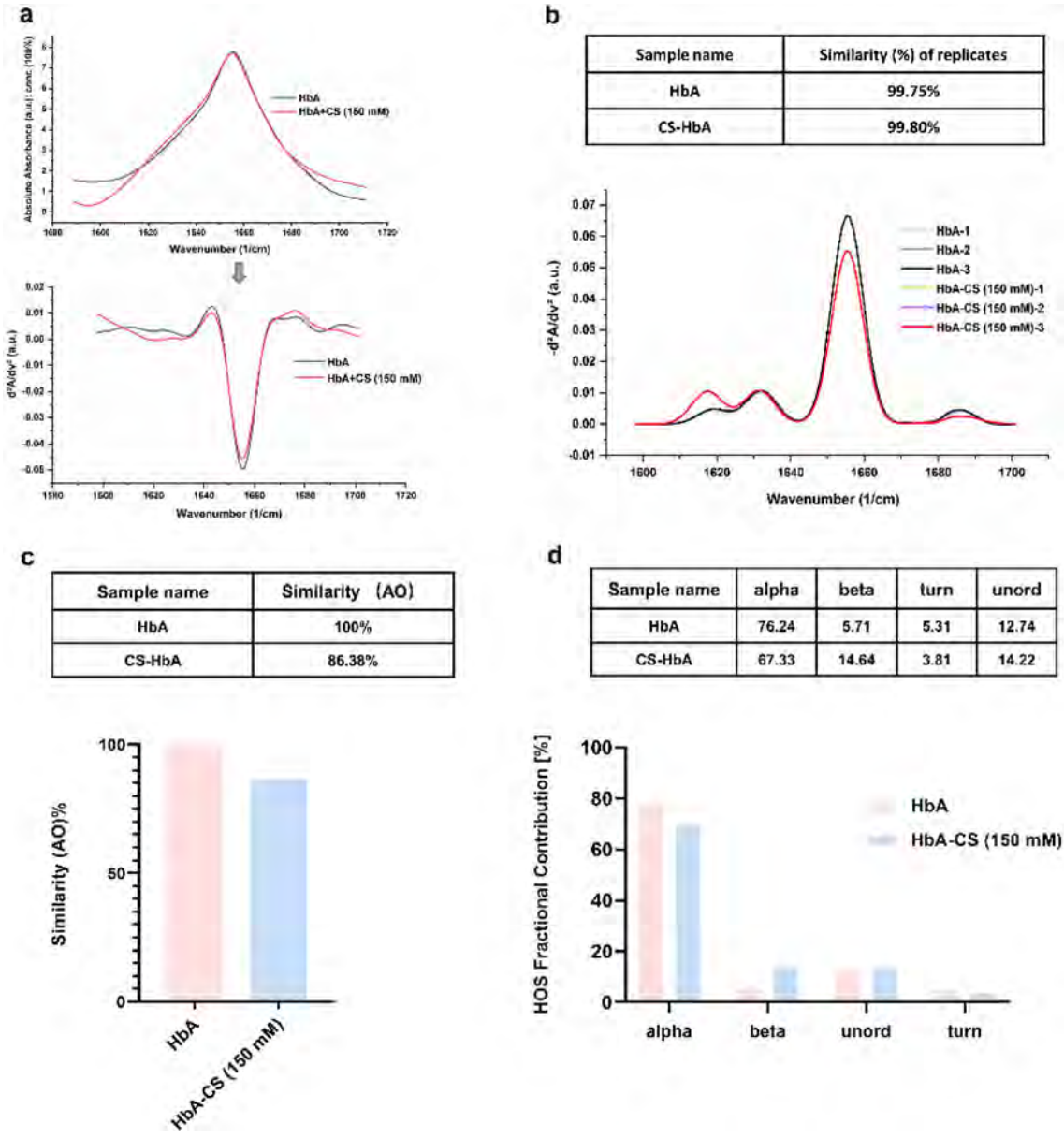

Figure 5. Cefmetazole sodium altered the secondary structure of HbA. (a) Convert the absolute absorption spectrum to the second derivative. (b) HbA and HbA with cefmetazole sodium (150 mM) were tested and show 99.75% and 99.80% similarity, respectively, indicating the stable system. (c) The structure of cefmetazole sodium-HbA complex was significantly different from HbA. (d) Cefmetazole sodium changed the HOS of HbA. Specifically, the alpha-helix of HbA was significantly reduced and the beta-sheet was significantly increased.

structural deviations. The RMSD of HbA varied from 1 Å to 3 Å for 100 ns. The left image of Figure 7b showed the initial conformation, and the right image of Figure 7b showed the final conformation after the dynamic simulation. As the simulation went on, cefmetazole sodium moved from the middle of the pocket formed by the two beta chains to the upper left part of the pocket by the end of the simulation time (Figure 7b). The results in Figure 7c showed that the carboxyl group of Cefmetazole sodium formed a salt bridge with the K233 of HbA (original K225) side chain. In addition, cefmetazole sodium has hydrogen bond interaction with K510 (original K625) and A 283 (original 285) of HbA. For the estimation of binding energy, we have employed MM/GBSA calculations (Ghufran et al., 2020; Khan et al., 2021) shown in Table 1. The results showed that the major contribution of the total binding free energy (-30.00 ± 5.65 kcal/mol) of the system is from the ΔGvdw (van der Waals forces). The ΔGele (electrostatic attraction force) is quite large in system, but the ΔGpolar (polar solvent effect) almost completely cancels out the ΔGele. ΔGgas and ΔGsolv energy also cancel each other out.

Cefmetazole sodium and 2,3-DPG compete for binding to HbA

SPR and molecular docking showed that 2,3-DPG can affect the binding between cefmetazole sodium and HbA. The SPR assay results showed that cefmetazole sodium could compete with 2,3-DPG to bind HbA when the concentration of 2,3-DPG was 800 μM (Figure 8a). The docking results (Figure 8b) showed that there was a salt bridge between the endogenous 2,3-DPG and HbA. The K625, H286, H145, K225, and H545

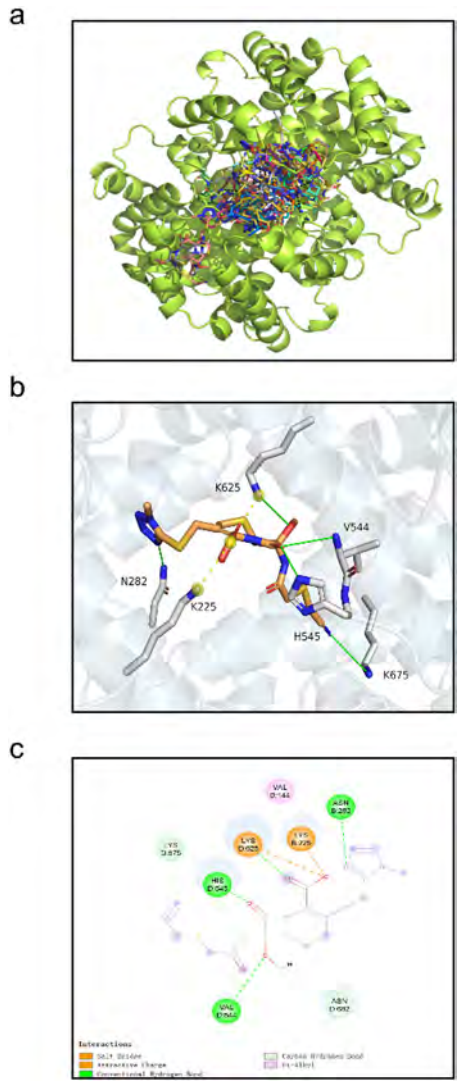

Figure 6. Specific binding mode of cefmetazole sodium and HbA. (a) The 100 possible conformations of the combination between cefmetazole sodium and HbA. (b) Diagram of the binding patterns between cefmetazole sodium and HbA with the lowest free energy. HbA: Silver gray, cartoon pattern; binding pocket amino acids: lgray, sticks; cefmetazole sodium: nitrogen atoms- blue sticks; oxygen atoms- red sticks: sulfur atoms- yellow sticks; HbA–cefmetazole sodium hydrogen bond: green solid line.;salt bridge interaction: yellow dotted line (c) The 2D diagram of HbA- cefmetazole sodium complex.

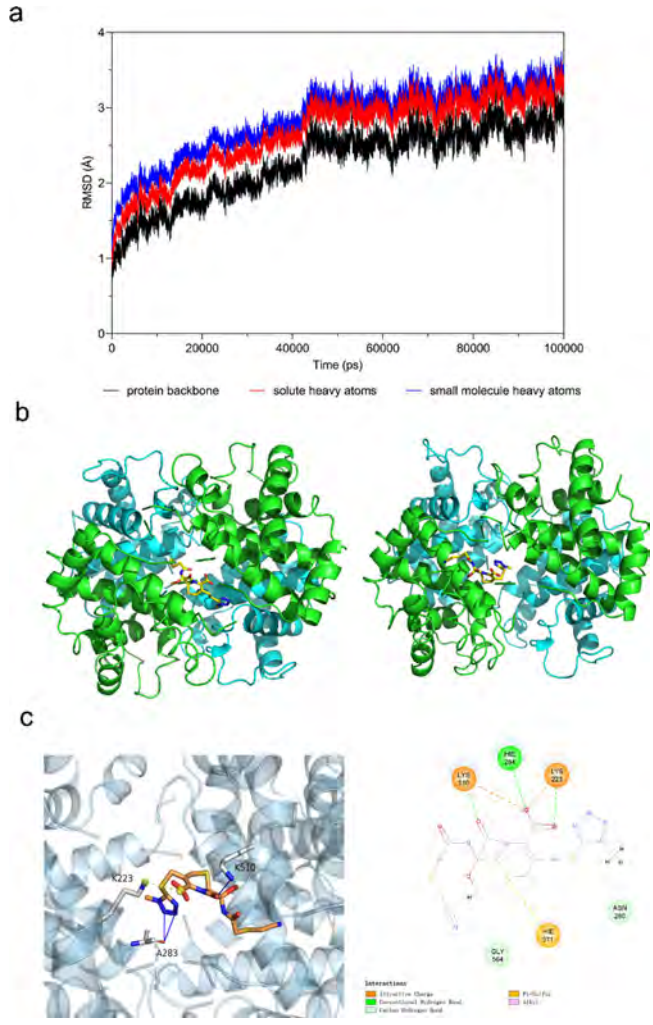

Figure 7. Cefmetazole sodium and HbA form a stable complex. (a) RMSD of HbA and cefmetazole sodium during 100 ns MD simulation. (b) After 100 ns of MD simulation, the position of cefmetazole sodium shifted slightly. α chain: blue; β chain: green; cefmetazole sodium: yellow small molecules. (c) HbA-cefmetazole sodium conformation in the last frame of MD simulation. 3D-Salt bridge interaction: yellow dotted line; 3D-hydrogen bonds: solid blue line.

Table 1. the MM/GBSA Binding free energy (kcal/mol) for HbA-cefmetazole sodium complex.

	Generalized born (GB)
ΔGvdw	−43.2450 ± 5.9519
ΔGele	−153.3670 ± 31.8741
ΔGpolar	172.6422 ± 30.1670
ΔGnonpolar	−6.0302 ± 0.6951
ΔGgas	−196.6120 ± 29.3123
ΔGsolv	166.6120 ± 30.4229
ΔGtotal	−30.0000 ± 5.6488

ΔGvdw, van der Waals energy; ΔGele, electrostatic energy; ΔGpolar, polar solvent effect; ΔGnonpolar, nonpolar solvation; ΔGgas, gas phase free energy; ΔGsol, solvation free energy.

residues of HbA (β-chain) formed hydrogen bonds network with 2,3-DPG. When bound to HbA, both cefmetazole sodium and endogenous 2,3-DPG were found in the same binding position, suggesting that they competitively bind to HbA. During the 100 ns molecular dynamics simulation of the 2,3-DPG-HbA complex, the RMSD of the entire system was analyzed as shown in Figure 8c. The protein backbone, all solute heavy atoms, and small molecule heavy atoms exhibited consistent variation trends. The RMSD value gradually increased and reached stability around 20 ns, with the RMSD variation remaining within 2. Figure 8d showed the final conformation after the dynamic simulation. The results of MM/GBSA binding free energy calculations of 2,3-DPG are presented in Table 2. The results indicated that the ΔGvdw made the most significant contribution to the overall binding free energy in this system. Although the ΔGele is notable in each system, it is largely balanced by the ΔGpolar. The ΔGgas and ΔGsolv energies also counteract each other. The ΔGtotal of 2,3-DPG with HbA is −14.3387 ± 30.4115 Kcal/mol, which is significantly lower than that of cefmetazole sodium with HbA (-30.0000 ± 5.6488 Kcal/mol, Table 1). Consequently, cefmetazole sodium and endogenous 2,3-DPG compete for binding to HbA (Figures 8b, 6c), while cefmetazole sodium exhibiting a stronger effect than 2,3-DPG.

Discussion

Oxygen is absolutely vital for the human body. Hemoglobin, a protein found in red blood cells, enables the blood to effectively carry and release oxygen. It is accomplished through the binding of oxygen to hemoglobin in the lungs, followed by its dissociation in the tissues. The oxygen transport is mainly determined by the oxygen supply efficiency of hemoglobin, which can be characterized by the oxygen affinity (P_{50}), cooperative effect (the Hill coefficient), Bohr effect (SI), and the theoretical oxygen-release capacity (ΔSO_2). Regulating the oxygen supply efficiency of hemoglobin is an attractive strategy in multiple applications.

Many diseases are associated with inadequate oxygen supply to the tissues, including sickle cell anemia and cardiopulmonary diseases. Based on accumulated data, manipulating the oxygen supply efficiency of hemoglobin through allosteric effectors is hopeful to treat many diseases. Maintaining hemoglobin in the high oxygen affinity state has benefit in SCD because it can delay the polymerization of deoxygenated HbS (Herity et al., 2021). Furthermore, enhancing the oxygen affinity of hemoglobin has the potential to take up more oxygen from the air to alleviate hypoxemia associated with pulmonary diseases, such as pulmonary fibrosis (Dufu et al., 2017). On the contrary, decreasing the oxygen affinity of hemoglobin may be beneficial in cardiopulmonary diseases that require enhanced oxygen release to tissues. Therefore, various allosteric effectors of hemoglobin have been identified to either increase (5-HMF, tucaresol, GBT440, and GBT1118) or decrease [etaproxiral (RSR-13) and ITPP] oxygen affinity (Patel et al., 2018).

In recent years, the repurposing of drugs has been recognized as an effective and tangible strategy for drug research and development. Compared with new drug research and development, drug repurposing has the advantages of a shorter time, lower cost, and higher safety. In the present study, SPRi high-throughput screening was used to determine the existing drugs that bound to HbA. Among the 1338 studied drugs, we identified that cefmetazole sodium, a second-generation cephalosporin, not only was an antibacterial agent but also could combine with HbA in a concentration-dependent manner, which was further verified by SPR.

Cefmetazole sodium is a semisynthetic cephamycin antibiotic with broad-spectrum antibacterial activity that contains a triazole ring and a benzodioxine group (Schentag, 1991) (Figure 2a). By binding penicillin-binding protein (PBP), a special protein on the bacterial cell serous membrane, cefmetazole sodium causes the loss of cell wall integrity and prevents the crosslinking of peptidoglycans. The active center of bacterial PBP is usually serine. β-Lactam antibiotics act by covalently combining the carboxyl group in the β-lactam ring with the hydroxyl group of serine in the bacterial PBP. In addition, the 7α-methoxy group of cefmetazole sodium sterically hinders the approach of β-lactamase. Therefore, drug resistance can be prevented to a certain extent (Schentag, 1991; Simada, 1995). However, no studies have reported an interaction between cefmetazole sodium and HbA. Our data shows cefmetazole sodium bound to HbA with a KD value of 5.82×10^{-4}, which is similar to the KD value of 2,3-DPG binding to HbA (4.62×10^{-4}). These results indicated that cefmetazole sodium and 2,3-DPG have similar binding force with HbA.

To further study the effect of this interaction, we investigated the effects of cefmetazole sodium on the function of HbA. According to the ODC, cefmetazole sodium could increase the HbA P_{50} value (reduced oxygen affinity), decrease the Hill coefficient and enhance the theoretical oxygen-release capacity in simulated plain and plateau conditions. That is, cefmetazole sodium could regulate the oxygen supply efficiency of HbA.

The physiological and clinical significance of increasing oxygen supply by increasing the P_{50} value has been investigated in many studies. Li has found that the P_{50} value increased compensatively when people moved from the plains to live at higher altitude (the plateau) without an acclimatization period (Li et al., 2018), which possibly resulted in an increased oxygen supply to the tissues. Valeri and Zaroulis have developed a technique to rejuvenate red blood cells by adding pyruvate, inosine, glucose, adenine and phosphate to stored blood. The P_{50} values of the stored blood were significantly improved to normal levels after rejuvenation, which can effectively reduce organ damage caused by blood transfusion through enhancing the oxygen supply of the stored blood (Woźniak et al., 2018; Srinivasan et al., 2018; Imai, 1982). Studies have shown that RSR-13 (300 mg/kg) significantly reduced hemoglobin oxygen affinity and increased tissue pO_2 values (Khandelwal et al., 1993). ITPP can enhance oxygen delivery and markedly shifted the ODC to the right and increased the P_{50} values both *in vitro* and *in vivo*. In addition, ITPP significantly enhances oxygen release of red blood cells (RBCs), demonstrating remarkable effects in the treatment of cardiovascular diseases and cancer (Duarte et al., 2010). Thus, the regulation of oxygen affinity, as mentioned earlier, may be useful in many clinical conditions.

Pharmacological interventions that target oxygen affinity may also impact the Hill coefficient (Bellelli & Tame, 2022), as observed in this study, wherein a decreased Hill coefficient suggests a weakening of the cooperative effect. However, it is not accompanied by the significance of the oxygen-saturated condition. Under physiological or near-physiological conditions, HbA has maximum synergism, with the Hill coefficient close to 3 (Imai, 1982). Pharmacological interventions that alter the Hill coefficient may be viewed as undesirable from a clinical viewpoint (Bellelli & Tame, 2022). Under resting conditions, the oxygen saturation of HbA ranges between 100% in the lungs and 70% in the tissues, which may drop to 50% with activity (Schmidt-Nielsen, 1975), but only during extreme activity do skeletal muscles need to extract large amounts of oxygen from the blood. According to Andrea Bellelli, the maximum value of the Hill coefficient is meaningful only in certain tissues and under extreme conditions (Bellelli & Tame, 2022). Thus, drug-induced Hill coefficient reductions are likely to be irrelevant in practice.

Satisfactorily, the results of the present study showed that cefmetazole sodium had little effect on the SI. The SI is an indicator of the Bohr effect, which is essential for the

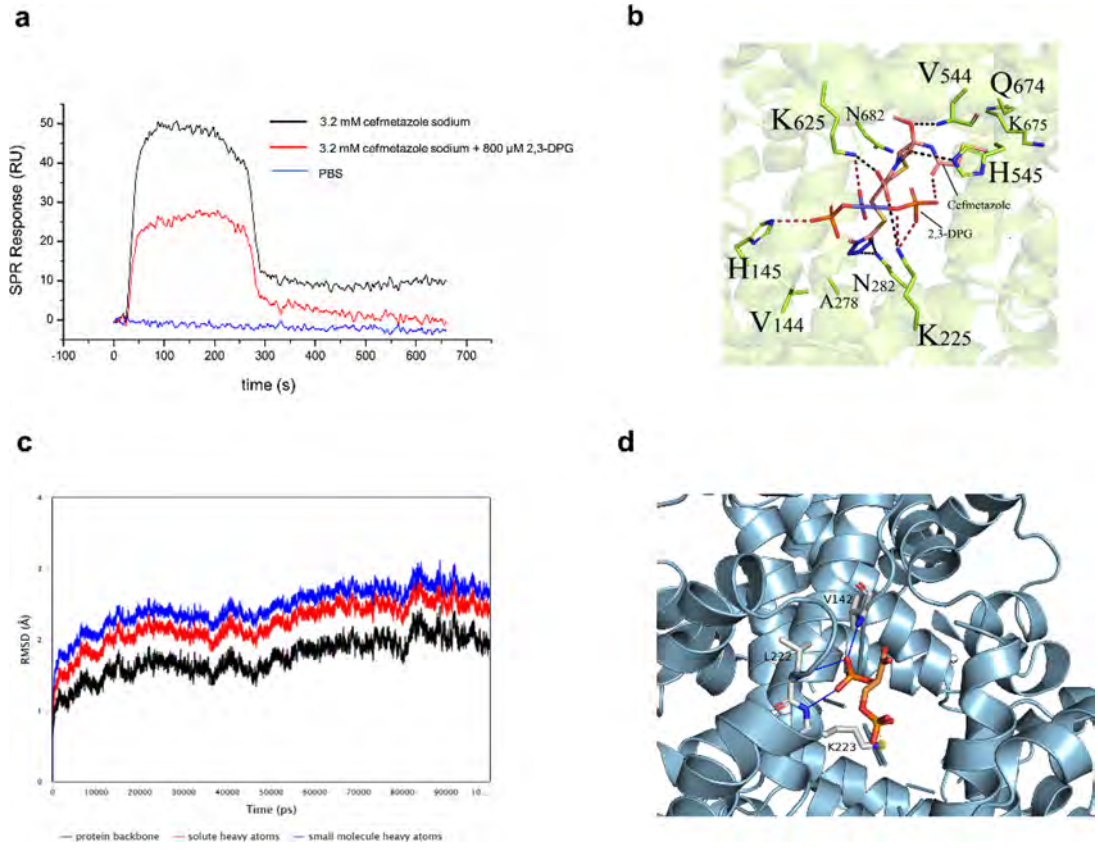

Figure 8. Competition between cefmetazole sodium and 2,3-DPG. (a) The 2,3-DPG weakened the binding ability of cefmetazole sodium to HbA, which was confirmed by surface plasmon resonance (SPR). (b) molecular docking showed that 2,3-DPG could compete with cefmetazole sodium in binding to HbA. HbA–cefmetazole sodium hydrogen bond: black dotted line; HbA–2,3-DPG hydrogen bond: brown dotted line. (c) RMSD of HbA and 2,3-DPG during 100 ns MD simulation. (d) HbA-cefmetazole sodium conformation in the last frame of MD simulation. 3D-Salt bridge interaction: yellow dotted line; 3D-hydrogen bonds: solid blue line.

Table 2. the MM/GBSA Binding free energy (kcal/mol) calculation for HbA-2,3-DPG complex.

	Generalized Born (GB)
ΔGvdw	−10.0549 ± 4.0572
ΔGele	−507.7920 ± 66.5409
ΔGpolar	505.7601 ± 62.9655
ΔGnonpolar	−2.1145 ± 0.3773
ΔGgas	−517.8470 ± 67.1316
ΔGsolv	503.6456 ± 62.7425
ΔGtotal	−14.2014 ± 7.2572

modulation of oxygen loading and unloading from the lungs to tissues. The Bohr effect reflects the ability of hemoglobin to bind oxygen in an alkaline environment and release oxygen in an acidic environment. However, other allosteric effectors, such as GBT440, have been reported to reduce the Bohr effect (Ming1, et al., 2020). Therefore, cefmetazole sodium demonstrates significant advantages over other allosteric effectors which reduce the Bohr effect of hemoglobin.

Cefmetazole sodium increased the theoretical oxygen-release capacity of HbA more significantly in a simulated plain area than that in a simulated plateau area. The possible reason is that high altitude areas are characterized by a low oxygen partial pressure. Cefmetazole sodium decreases the oxygen affinity of HbA, resulting in less oxygen uptake under the condition with lower oxygen partial pressure. ODA experiments showed that cefmetazole sodium could accelerate the oxygen release of HbA, possibly because cefmetazole sodium keep HbA in T-state. Therefore, the administration of cefmetazole sodium may lead to increased oxygen delivery to peripheral tissues.

Understanding the secondary structure of proteins is crucial for unraveling their functionality and stability (Rost, 2001; Xie & Schowen, 1999). The higher order structure (HOS) of proteins is predominantly determined by intramolecular hydrogen bonds between the amine hydrogen and carbonyl oxygen atoms in the peptide backbone. It plays a crucial role in dictating the folding pattern of peptide units and the overall conformation of protein molecules (Jin et al., 2023). To investigate the secondary structure changes of HbA induced by cefmetazole sodium, we utilized MMS to find a conversion of the alpha-helix conformation to the beta-sheet structure. The HbA secondary structural changes with the hydrophobic action and hydrogen bonding. Cefmetazole sodium binding may expose some groups inside the beta-sheet, which leads to the transformation of the alpha-helix of HbA to the beta-sheet (Shibayama, 2020). This process is accompanied by a stable aggregation process of intermolecular hydrogen bonds. The stability of hydrogen bond may lead to the transformation of HbA from 'R' state to 'T' state and enhance the oxygen-releasing capacity of HbA, which is consistent with previous results. It is reported that the transition from the R-state to T-state of HbA is accompanied by the breaking and formation of salt bridges at the α1/β2 and α2/β1 interfaces, along with changes in local hydrophobicity. In the T-state, more water entrances the central water cavity

through the β-cleft narrows (Pezzella et al., 2020; Latypova et al., 2020). Therefore, cefmetazole sodium may weaken the hydrophobicity of HbA.

Molecular docking analysis was conducted to explore how cefmetazole sodium regulated the HbA oxygen supply efficiency. The 2,3-DPG was subjected to a redocking process, and the RMSD value was 1.006 Å. Docking results are generally considered accurate if the RMSD relative to the native pose is $\leq$ 2.0 Å (Li et al., 2011). The docking data indicated that cefmetazole sodium specifically bound with the N282, K225, H545, K625, K675 and V544 amino acid residues of the β chains of HbA, and the binding energy was −7.32 kcal/mol, which indicated a strong binding. Asnβ139 (N282), Hisβ2 (H545), and Lysβ82 (K225/K625) were key residues for HbA binding to 2,3-DPG. These residues have been reported to be crucial for the regulation of hemoglobin oxygen affinity (Ahmed et al., 2020). Hisβ2 (H545) and Lysβ82 (K225/K625) are part of the H^+ binding sites (Ahmed et al., 2020) and Lysβ82 (K255/K625) is a part of the Cl^- binding sites (Ahmed et al., 2020; Fronticelli et al., 1994; Perutz et al., 1993). Valβ1 (V544) and Lysβ82 (K255/K625) form part of the site for pyridoxal 5-phosphatemonohydrate modification of hemoglobin-based oxygen carriers (Alayash, 2014). Notably, binding to N282, K225, H545, K625, and V544 always increases the hemoglobin P_{50} value, regardless of the type of allosteric effector (Ahmed et al., 2020). Significantly, the interaction of cefmetazole sodium with bHb, which lacks Valβ1 and Hisβ2 residues, did not increase the P_{50} value (support information). This result further indicated that Valβ1 and Hisβ2 are the key sites affecting the oxygen affinity of HbA.

The carboxylic acid on the 6-membered ring, the methoxy and carbonyl groups on the azabicyclo[4.2.0] core, and the nitrogens at the 3- and 4-positions of the tetrazole moiety of cefmetazole sodium are the main groups that bind to HbA. Among them, the carboxylic acid on the 6-membered ring is responsible for the bactericidal action because this acid group can covalently combine with the serine hydroxyl group of PBP to form a serine ester, which inhibits the synthesis of the cell wall of bacterial. The presence of the trans-methoxy group on the β-lactam ring results in a sterically hindered structure and is an important group for preventing bacterial resistance to cefmetazole (Schentag, 1991; Araki et al., 2019). The present results suggest that all cephalosporins with a similar 7-amino cephalosporin (7-ACA) structure may have a similar effect to that of cefmetazole because their parent nucleus may be able to bind to HbA and regulate oxygen supply efficiency.

Docking alone is insufficient to provide a complete understanding of the binding mode, stability, and dynamics of potential ligands. Therefore, we conducted MD simulations for various nano-second frames using the stable complexes obtained from docking HbA with cefmetazole sodium. This approach allows us to gain further insight into the binding interactions and assess the stability of the complexes over time. The molecular dynamics simulation revealed a tight binding of cefmetazole sodium with the binding pocket of HbA. The protein-ligand complex maintains stability throughout the 100 ns duration of the MD simulation, as evidenced by a low RMSD value. This observation suggests that the docked complex is structurally stable over time, primarily due to the presence of hydrogen bonds and van der Waals interactions. During the simulation, the shift of RMSD in the order of 1 Å–3 Å indicate that the whole system has undergone moderate conformational changes. The binding free energies of HbA-cefmetazole sodium has been precisely predicted using MM/GBSA (Ghufran et al., 2020; Khan et al., 2021). The summation of nonpolar solvation free energy and polar solvation free energy is termed as ΔGsolv score, which is dependent on the solvation method employed. Similarly, ΔGgas score represents the sum of van der Waals contributions and electrostatic interactions from the molecular mechanics force field, and it is independent of the solvation model used. The overall binding free energies of the complexes was −30.00 ± 5.65 kcal/mol, indicating that the complex was stable (Irfan et al., 2023).

The 2,3-DPG is an important endogenous allosteric effector that can bind to HbA in red blood cells to stabilize the 'T' state of HbA and reduce oxygen affinity. Patients with chronic hypoxemia have shown physiological increases in 2,3-DPG, which enhanced oxygen release to meet the oxygen demands of tissues (Koizumi, 1991). In our study, we employed a combination of surface plasmon resonance (SPR) and molecular docking techniques to investigate the binding ability of cefmetazole sodium to HbA in the presence of endogenous 2,3-DPG interference. The docking results showed that there was a salt bridge system between the endogenous 2,3-DPG and HbA. K625, H286, H145, K225, and H545 residues of the HbA β-chain formed hydrogen bonds with 2,3-DPG to constitute a hydrogen bonding network. Cefmetazole sodium and endogenous 2,3-DPG were located in the same central water cavity when bounding to HbA simultaneously, which suggesting that the two compounds bind with HbA competitively. The binding constant is essential to verify the interaction between cefmetazole sodium and HbA *in vivo* (Chamani et al., 2005; Hosseinzadeh et al., 2019). The KD value of cefmetazole sodium binding to HbA was 5.82×10^{-4}, which is similar to the KD value of 2,3-DPG binding to HbA (4.62×10^{-4}). It's reported that the concentration of 2,3-DPG *in vivo* is 0.83 mol·mol^{-1} Hb under physiological conditions (Odje & Ramsey, 1995). However, in our SPR study, the concentration of 2,3-DPG was 10.88 mol.mol^{-1} Hb, which was much higher. And under this condition cefmetazole sodium still could decrease the binding between 2,3-DPG and HbA. Furthermore, the ΔGtotal of cefmetazole sodium with HbA is −30.0000 ± 5.6488 kcal/mol, which is significantly higher than that of 2,3-DPG with HbA (-14.3387 ± 30.4115 kcal/mol). These data suggests that cefmetazole sodium can bind to HbA and regulate the oxygen supply efficiency under physiological conditions.

Conclusion

Cefmetazole sodium, an antibacterial drug, was found to also act as an allosteric effector that can interact with HbA to form a stable complex, leading to alterations in its secondary structure and regulation of its oxygen supply efficiency (no significant effect on bHb was observed). The amino acid

residues of HbA—N282, K225, H545, K625, K675 and V544—may be the key binding sites for the targeted increase in the P_{50} value. Other ligands with 7-ACA as the parent nucleus may also be capable of binding HbA and regulating oxygen supply efficiency. In addition, cefmetazole sodium exhibited a higher binding affinity than 2,3-DPG, indicating the potential regulatory effect of cefmetazole sodium *in vivo*.

Funding

The author(s) reported there is no funding associated with the work featured in this article.

References

Ahmed, M. H., Ghatge, M. S., & Safo, M. K. (2020). Hemoglobin: Structure, function and allostery. *Sub-Cellular Biochemistry*, *94*, 345–382. https://doi.org/10.1007/978-3-030-41769-7_14

Alayash, A. I. (2014). Blood substitutes: Why haven't we been more successful? *Trends in Biotechnology*, *32*(4), 177–185. https://doi.org/10.1016/j.tibtech.2014.02.006

Aprahamian, M., Bour, G., Akladios, C. Y., Fylaktakidou, K., Greferath, R., Soler, L., Marescaux, J., Egly, J.-M., Lehn, J.-M., & Nicolau, C. (2011). Myo-InositolTrisPyroPhosphate treatment leads to HIF-1α suppression and eradication of early hepatoma tumors in rats. *Chembiochem : A European Journal of Chemical Biology*, *12*(5), 777–783. https://doi.org/10.1002/cbic.201000619

Araki, K., Fukuoka, K., Higuchi, H., Aizawa, Y., & Horikoshi, Y. (2019). Cefmetazole for extended-spectrum β-lactamase-producing Enterobacteriaceae in pediatric pyelonephritis. *Pediatrics International : official Journal of the Japan Pediatric Society*, *61*(6), 572–577. https://doi.org/10.1111/ped.13847

Assaran Darban, R., Shareghi, B., Asoodeh, A., & Chamani, J. (2017). Multi-spectroscopic and molecular modeling studies of interaction between two different angiotensin I converting enzyme inhibitory peptides from gluten hydrolysate and human serum albumin. *Journal of Biomolecular Structure & Dynamics*, *35*(16), 3648–3662. https://doi.org/10.1080/07391102.2016.1264892

Bellelli, A., & Tame, J. R. H. (2022). Hemoglobin allostery and pharmacology. *Molecular Aspects of Medicine*, *84*, 101037. https://doi.org/10.1016/j.mam.2021.101037

Benner, A., Patel, A. K., Singh, K., & Dua, A. (2022). Physiology, Bohr Effect. In: *StatPearls*. StatPearls Publishing LLC.

Blair, H. A. (2020). Voxelotor: First approval. *Drugs*, *80*(2), 209–215. https://doi.org/10.1007/s40265-020-01262-7

Bunn, H. F. (1997). Pathogenesis and treatment of sickle cell disease. *The New England Journal of Medicine*, *337*(11), 762–769. https://doi.org/10.1056/NEJM199709113371107

Carreau, A., El Hafny-Rahbi, B., Matejuk, A., Grillon, C., & Kieda, C. (2011). Why is the partial oxygen pressure of human tissues a crucial parameter? Small molecules and hypoxia. *Journal of Cellular and Molecular Medicine*, *15*(6), 1239–1253. https://doi.org/10.1111/j.1582-4934.2011.01258.x

Chamani, J., Moosavi-Movahedi, A. A., & Hakimelahi, G. H. (2005). Structural changes in β-lactoglobulin by conjugation with three different kinds of carboxymethyl cyclodextrins. *Thermochimica Acta*, *432*(1), 106–111. https://doi.org/10.1016/j.tca.2005.04.014

Chu, Z., Wang, Y., You, G., Wang, Q., Ma, N., Li, B., Zhao, L., & Zhou, H. (2020). The P50 value detected by the oxygenation-dissociation analyser and blood gas analyser. *Artificial Cells, Nanomedicine, and Biotechnology*, *48*(1), 867–874. https://doi.org/10.1080/21691401.2020.1770272

Coll-Satue, C., Jansman, M. M. T., Thulstrup, P. W., & Hosta-Rigau, L. (2021). Optimization of Hemoglobin encapsulation within PLGA nanoparticles and their investigation as potential oxygen carriers. *Pharmaceutics*, *13*(11), 1958. https://doi.org/10.3390/pharmaceutics13111958

Derbal-Wolfrom, L., Pencreach, E., Saandi, T., Aprahamian, M., Martin, E., Greferath, R., Tufa, E., Choquet, P., Lehn, J.-M., Nicolau, C., Duluc, I., & Freund, J.-N. (2013). Increasing the oxygen load by treatment with myo-inositol trispyrophosphate reduces growth of colon cancer and modulates the intestine homeobox gene Cdx2. *Oncogene*, *32*(36), 4313–4318. https://doi.org/10.1038/onc.2012.445

Duarte, C. D., Greferath, R., Nicolau, C., & Lehn, J. M. (2010). myo-Inositol trispyrophosphate: A novel allosteric effector of hemoglobin with high permeation selectivity across the red blood cell plasma membrane. *Chembiochem : a European Journal of Chemical Biology*, *11*(18), 2543–2548. https://doi.org/10.1002/cbic.201000499

Dufu, K., Yalcin, O., Ao-leong, E. S. Y., Hutchaleelala, A., Xu, Q., Li, Z., Vlahakis, N., Oksenberg, D., Lehrer-Graiwer, J., & Cabrales, P. (2017). GBT1118, a potent allosteric modifier of hemoglobin O(2) affinity, increases tolerance to severe hypoxia in mice. *American Journal of Physiology. Heart and Circulatory Physiology*, *313*(2), H381–H391. https://doi.org/10.1152/ajpheart.00772.2016

Dybas, J., Bokamper, M. J., Marzec, K. M., & Mak, P. J. (2020). Probing the structure-function relationship of hemoglobin in living human red blood cells. *Spectrochimica Acta. Part A, Molecular and Biomolecular Spectroscopy*, *239*, 118530. https://doi.org/10.1016/j.saa.2020.118530

Eaton, W. A., & Hofrichter, J. (1990). Sickle cell hemoglobin polymerization. *Advances in Protein Chemistry*, *40*, 63–279. https://doi.org/10.1016/s0065-3233(08)60287-9

Fronticelli, C., Pechik, I., Brinigar, W. S., Kowalczyk, J., & Gilliland, G. L. (1994). Chloride ion independence of the Bohr effect in a mutant human hemoglobin beta (V1M + H2deleted). *J Biol Chem*,.*269*(39), 23965–23969. https://doi.org/10.1016/S0021-9258(19)51032-8

Fylaktakidou, K. C., Lehn, J. M., Greferath, R., & Nicolau, C. (2005). Inositol tripyrophosphate: A new membrane permeant allosteric effector of haemoglobin. *Bioorganic & Medicinal Chemistry Letters*, *15*(6), 1605–1608. https://doi.org/10.1016/j.bmcl.2005.01.064

Ghufran, M., Rehman, A. U., Shah, M., Ayaz, M. A.-O., Ng, H. L., & Wadood, A. (2020). In-silico design of peptide inhibitors of K-Ras target in cancer disease. *Journal of Biomolecular Structure & Dynamics*, *38*(18), 5488–5499. https://doi.org/10.1080/07391102.2019.1704880

Giardina, B., Messana, I., Scatena, R., & Castagnola, M. (1995). The multiple functions of hemoglobin. *Critical Reviews in Biochemistry and Molecular Biology*, *30*(3), 165–196. https://doi.org/10.3109/10409239509085142

Herity, L. B., Vaughan, D. M., Rodriguez, L. R., & Lowe, D. K. (2021). Voxelotor: A novel treatment for sickle cell disease. *The Annals of Pharmacotherapy*, *55*(2), 240–245. https://doi.org/10.1177/1060028020943059

Hill, R. J., Konigsberg, W., Guidotti, G., & Craig, L. C. (1962). The structure of human hemoglobin. I. The separation of the alpha and beta chains and their amino acid composition. *The Journal of Biological Chemistry*, *237*, 1549–1554.

Hosseinzadeh, M., Nikjoo, S., Zare, N., Delavar, D., Beigoli, S., & Chamani, J. (2019). Characterization of the structural changes of human serum albumin upon interaction with single-walled and multi-walled carbon nanotubes: Spectroscopic and molecular modeling approaches. *Research on Chemical Intermediates*, *45*(2), 401–423. https://doi.org/10.1007/s11164-018-3608-5

Imai, K. (1982). The molecular mechanism of allosteric effects in hemoglobin (author's transl). *Seikagaku*, *54*(4),197-26.

Irfan, A. A.-O., Faisal, S. A.-O., Ahmad, S. A.-O., Al-Hussain, S. A., Javed, S. A.-O., Zahoor, A. A.-O., et al. (2023). Structure-based virtual screening of furan-1,3,4-oxadiazole tethered N-phenylacetamide derivatives as novel class of hTYR and hTYRP1 inhibitors. *Pharmaceuticals (Basel)*, *16*(3), 344. https://doi.org/10.3390/ph16030344

Ivancic, V. A., Lombardo, H. L., Ma, E., Wikström, M., & Batabyal, D. (2022). Advancing secondary structure characterization of monoclonal antibodies using Microfluidic Modulation Spectroscopy. *Analytical Biochemistry*, *646*, 114629. https://doi.org/10.1016/j.ab.2022.114629

Jin, C., Patel, A., Peters, J., Hodawadekar, S., & Kalyanaraman, R. A.-O. (2023). Quantum cascade laser based infrared spectroscopy: A new paradigm for protein secondary structure measurement. *Pharmaceutical Research*, *40*(6), 1507–1517.https://doi.org/10.1007/s11095-022-03422-8 Epub ahead of print.

Kaufman, D. P., Kandle, P. F., Murray, I., & Dhamoon, A. S. (2022). Physiology, oxyhemoglobin dissociation curve. In: *StatPearls*. StatPearls Publishing LLC.

Khan, A., Umbreen, S., Hameed, A., Fatima, R., Zahoor, U., Babar, Z., Waseem, M., Hussain, Z., Rizwan, M., Zaman, N., Ali, S., Suleman, M., Shah, A., Ali, L., Ali, S. S., & Wei, D.-Q. (2021). In Silico mutagenesis-based remodelling of SARS-CoV-1 peptide (ATLQAIAS) to inhibit SARS-CoV-2: structural-dynamics and free energy calculations. *Interdisciplinary Sciences, Computational Life Sciences*, *13*(3), 521–534. https://doi.org/10.1007/s12539-021-00447-2

Khandelwal, S. R., Randad, R. S., Lin, P. S., Meng, H., Pittman, R. N., Kontos, H. A., Choi, S. C., Abraham, D. J., & Schmidt-Ullrich, R. (1993). Enhanced oxygenation in vivo by allosteric inhibitors of hemoglobin saturation. *The American Journal of Physiology*, *265*(4 Pt 2), H1450–3. https://doi.org/10.1152/ajpheart.1993.265.4.H1450

Khashkhashi-Moghadam, S., Ezazi-Toroghi, S., Kamkar-Vatanparast, M., Jouyaeian, P., Mokaberi, P., Yazdyani, H., Amiri-Tehranizadeh, Z., Reza Saberi, M., & Chamani, J. (2022). Novel perspective into the interaction behavior study of the cyanidin with human serum albumin-holo transferrin complex: Spectroscopic, calorimetric and molecular modeling approaches. *Journal of Molecular Liquids*, *356*, 119042. https://doi.org/10.1016/j.molliq.2022.119042

Koizumi, M. (1991). Oxyhemoglobin dissociation curve and 2,3-diphosphoglycerate in chronic hypoxemia. *Nihon Kyobu Shikkan Gakkai Zasshi*, *29*(5), 547–553.

Latypova, L. A.-O., Barshtein, G. A.-O., Puzenko, A., Poluektov, Y., Anashkina, A., Petrushanko, I., et al. (2020). Oxygenation state of hemoglobin defines dynamics of water molecules in its vicinity. *Journal of Chemical Physics*. *153*(13), 135101.

Li, J., Abel R Fau- Zhu, K., Zhu, K., Fau- Cao, Y., Cao, Y., Fau- Zhao, S., Zhao, S., Fau- Friesner, R. A., & Friesner, R. A. (2011). The VSGB 2.0 model: A next generation energy model for high resolution protein structure modeling. *Proteins*, *79*(10), 2794–2812. https://doi.org/10.1002/prot.23106

Li, C., Li, X., Liu, J., Fan, X., You, G., Zhao, L., Zhou, H., Li, J., & Lei, H. (2018). Investigation of the differences between the Tibetan and Han populations in the hemoglobin-oxygen affinity of red blood cells and in the adaptation to high-altitude environments. *Hematology (Amsterdam, Netherlands)*, *23*(5), 309–313. https://doi.org/10.1080/10245332.2017.1396046

Limani, P., Linecker, M., Kachaylo, E., Tschuor, C., Kron, P., Schlegel, A., Ungethuem, U., Jang, J. H., Georgiopoulou, S., Nicolau, C., Lehn, J.-M., Graf, R., Humar, B., & Clavien, P.-A. (2016). Antihypoxic potentiation of standard therapy for experimental colorectal liver metastasis through myo-inositol trispyrophosphate. *Clinical Cancer Research : An Official Journal of the American Association for Cancer Research*, *22*(23), 5887–5897. https://doi.org/10.1158/1078-0432.CCR-15-3112

Li, Y., Xiong, Y., Wang, R., Tang, F., & Wang, X. (2016). Blood banking-induced alteration of red blood cell oxygen release ability. *Blood Transfus*, *14*, 238–244.

Mairbäurl, H., & Weber, R. E. (2012). Oxygen transport by hemoglobin. *Comprehensive Physiology*, *2*(2), 1463–1489. https://doi.org/10.1002/cphy.c080113

Malte, H., & Lykkeboe, G. (2018). The Bohr/Haldane effect: A model-based uncovering of the full extent of its impact on O(2) delivery to and CO(2) removal from tissues. *Journal of Applied Physiology (Bethesda, Md. : 1985)*, *125*(3), 916–922. https://doi.org/10.1152/japplphysiol.00140.2018

Ming, , W., Jian, H., Yu, C., Wenting, S., Xiaoxu, L., Libin, G., et al. (2020). Effect of GBT440 on oxygen-carrying characteristics and its anti-hypoxia effect in hypoxia animal model. *The Youth Training Plan of Military Medical Science and Technology*, *42*, 923–928.

Nakagawa, A., Ferrari, M., Schleifer, G., Cooper, M. K., Liu, C., Yu, B., Berra, L., Klings, E. S., Safo, R. S., Chen, Q., Musayev, F. N., Safo, M. K., Abdulmalik, O., Bloch, D. B., & Zapol, W. M. (2018). A triazole disulfide compound increases the affinity of hemoglobin for oxygen and reduces the sickling of human sickle cells. *Molecular Pharmaceutics*, *15*(5), 1954–1963. https://doi.org/10.1021/acs.molpharmaceut.8b00108

Odje, O. E., & Ramsey, J. M. (1995). Effect of short-term strenuous exercise on erythrocyte 2,3-diphosphoglycerate in untrained men: a time-course study. *European Journal of Applied Physiology and Occupational Physiology*, *71*(1), 53–57. https://doi.org/10.1007/BF00511232

Patel, M. P., Siu, V., Silva-Garcia, A., Xu, Q., Li, Z., & Oksenberg, D. (2018). Development and validation of an oxygen dissociation assay, a screening platform for discovering, and characterizing hemoglobin-oxygen affinity modifiers. *Drug Design, Development and Therapy*, *12*, 1599–1607. https://doi.org/10.2147/DDDT.S157570

Perutz, M. F., Fermi, G., Poyart, C., Pagnier, J., & Kister, J. (1993). A novel allosteric mechanism in haemoglobin. Structure of bovine deoxyhaemoglobin, absence of specific chloride-binding sites and origin of the chloride-linked Bohr effect in bovine and human haemoglobin. *Journal of Molecular Biology*, *233*(3), 536–545. https://doi.org/10.1006/jmbi.1993.1530

Perutz, M. F., & TenEyck, L. F. (1972). Stereochemistry of cooperative effects in hemoglobin. *Cold Spring Harbor Symposia on Quantitative Biology*, *36*, 295–310. https://doi.org/10.1101/sqb.1972.036.01.040

Perutz, M. F., Wilkinson, A. J., Paoli, M., & Dodson, G. G. (1998). The stereochemical mechanism of the cooperative effects in hemoglobin revisited. *Annual Review of Biophysics and Biomolecular Structure*, *27*, 1–34. https://doi.org/10.1146/annurev.biophys.27.1.1

Pezzella, M., El Hage, K., Niesen, M. J. M., Shin, S., Willard, A. P., Meuwly, M., & Karplus, M. (2020). Water Dynamics Around Proteins: T- and R-States of Hemoglobin and Melittin. *The Journal of Physical Chemistry. B*, *124*(30), 6540–6554. https://doi.org/10.1021/acs.jpcb.0c04320

Raykov, Z., Grekova, S. P., Bour, G., Lehn, J. M., Giese, N. A., Nicolau, C., & Aprahamian, M. (2014). Myo-inositol trispyrophosphate-mediated hypoxia reversion controls pancreatic cancer in rodents and enhances gemcitabine efficacy. *International Journal of Cancer*, *134*(11), 2572–2582. https://doi.org/10.1002/ijc.28597

Rees, D. C., Williams, T. N., & Gladwin, M. T. (2010). Sickle-cell disease. *Lancet (London, England)*, *376*(9757), 2018–2031. https://doi.org/10.1016/S0140-6736(10)61029-X

Rost, B. (2001). Review: Protein secondary structure prediction continues to rise. *Journal of Structural Biology*, *134*(2-3), 204–218. https://doi.org/10.1006/jsbi.2001.4336

Safo, M. K., Ahmed, M. H., Ghatge, M. S., & Boyiri, T. (2011). Hemoglobin-ligand binding: Understanding Hb function and allostery on atomic level. *Biochimica et Biophysica Acta*, *1814*(6), 797–809. https://doi.org/10.1016/j.bbapap.2011.02.013

Schentag, J. J. (1991). Cefmetazole sodium: Pharmacology, pharmacokinetics, and clinical trials. *Pharmacotherapy*, *11*(1), 2–19.

Schmidt-Nielsen, K. (1975). Adaptation and environment. *Animal Physiology*, *22*(1), 1.

Sharifi-Rad, A., Mehrzad, J., Darroudi, M., Saberi, M. R., & Chamani, J. (2021). Oil-in-water nanoemulsions comprising Berberine in olive oil: Biological activities, binding mechanisms to human serum albumin or holo-transferrin and QMMD simulations. *Journal of Biomolecular Structure & Dynamics*, *39*(3), 1029–1043. https://doi.org/10.1080/07391102.2020.1724568

Shibayama, N. (2020). Allosteric transitions in hemoglobin revisited. *Biochimica et Biophysica Acta. General Subjects*, *1864*(2), 129335. https://doi.org/10.1016/j.bbagen.2019.03.021

Simada, D. (1995). Clinical value of cefmetazole and other cephamycin antibiotics. *Antibiotiki i Khimioterapiia = Antibiotics and Chemoterapy [Sic]*, *40*(1), 13–21.

Srinivasan, A. J., Kausch, K., Inglut, C., Gray, A., Landrigan, M., Poisson, J. L., Schroder, J. N., & Welsby, I. J. (2018). Estimation of achievable oxygen consumption following transfusion with rejuvenated red blood cells. *Seminars in Thoracic and Cardiovascular Surgery*, *30*(2), 134–141. https://doi.org/10.1053/j.semtcvs.2018.02.009

Srinivasan, A. J., Morkane, C., Martin, D. S., & Welsby, I. J. (2017). Should modulation of p50 be a therapeutic target in the critically ill? *Expert Review of Hematology*, *10*(5), 449–458. https://doi.org/10.1080/17474086.2017.1313699

Suh, J. H., Stea, B., Nabid, A., Kresl, J. J., Fortin, A., Mercier, J.-P., Senzer, N., Chang, E. L., Boyd, A. P., Cagnoni, P. J., & Shaw, E. (2006). Phase III study of efaproxiral as an adjunct to whole-brain radiation therapy for brain metastases. *Journal of Clinical Oncology : Official Journal of the American Society of Clinical Oncology*, *24*(1), 106–114. https://doi.org/10.1200/JCO.2004.00.1768

Taheri, R., Hamzkanlu, N., Rezvani, Y., Niroumand, S., Samandar, F., Amiri-Tehranizadeh, Z., Saberi, M. R., & Chamani, J. (2022). Exploring the HSA/DNA/lung cancer cells binding behavior of p-Synephrine, a

naturally occurring phenyl ethanol amine with anti-adipogenic activity: Multi spectroscopic, molecular dynamic and cellular approaches. *Journal of Molecular Liquids*, *368*, 120826. https://doi.org/10.1016/j.molliq.2022.120826

Woźniak, M. J., Qureshi, S., Sullo, N., Dott, W., Cardigan, R., Wiltshire, M., Nath, M., Patel, N. N., Kumar, T., Goodall, A. H., & Murphy, G. J. (2018). A comparison of red cell rejuvenation versus mechanical washing for the prevention of transfusion-associated organ injury in swine. *Anesthesiology*, *128*(2), 375–385. https://doi.org/10.1097/ALN.0000000000001973

Xie, M., & Schowen, R. L. (1999). Secondary structure and protein deamidation. *Journal of Pharmaceutical Sciences*, *88*(1), 8–13. https://doi.org/10.1021/js9802493

Xu, C.-P., Qi, Y., Cui, Z., Yang, Y.-J., Wang, J., Hu, Y.-J., Yu, B., Wang, F.-Z., Yang, Q.-P., & Sun, H.-T. (2019). Discovery of novel elongator protein 2 inhibitors by compound library screening using surface plasmon resonance. *RSC Advances*, *9*(3), 1696–1704. https://doi.org/10.1039/c8ra09640f

Yuan, Y., Tam, M. F., Simplaceanu, V., & Ho, C. (2015). New look at hemoglobin allostery. *Chemical Reviews*, *115*(4), 1702–1724. https://doi.org/10.1021/cr500495x

Zhong, Z. J., Hu, X. T., Cheng, L. P., Zhang, X. Y., Zhang, Q., & Zhang, J. (2021). Discovery of novel thiophene derivatives as potent neuraminidase inhibitors. *European Journal of Medicinal Chemistry*, *225*, 113762. https://doi.org/10.1016/j.ejmech.2021.113762